RSC Advances

PAPER

Cite this: *RSC Adv.*, 2019, **9**, 19065

Synthesis and biological evaluation of 4-(1*H*-1,2,4-triazol-1-yl)benzoic acid hybrids as anticancer agents†

Hatem A. Abuelizz,[a] Hanem M. Awad,[b] Mohamed Marzouk,[c] Fahd A. Nasr,[d] Ali S. Alqahtani,[e] Ahmed H. Bakheit,[af] Ahmed M. Naglah[gh] and Rashad Al-Salahi *[a]

A series of 4-(1*H*-1,2,4-triazol-1-yl)benzoic acid hybrids (**1–17**) was successfully synthesized and their structures were established by NMR and MS analysis. *In vitro* cytotoxic evaluation indicated that some of the hybrids exhibited potent inhibitory activities against MCF-7 and HCT-116 cancer cell lines, with IC_{50} values ranging from 15.6 to 23.9 μM, compared with reference drug doxorubicin (19.7 and 22.6 μM, respectively). Notably, the most potent compounds, **2**, **5**, **14**, and **15**, not only exhibited an obvious improvement in IC_{50} values, but demonstrated very weak cytotoxic effects toward normal cells (RPE-1) compared with doxorubicin. A further investigation showed that compounds **2** and **14** clearly inhibited the proliferation of MCF-7 cancer cells by inducing apoptosis. In addition, these hybrids showed acceptable correlation with bioassay results in regression plots generated by 2D QSAR models. Our results indicated that 1,2,4-triazole benzoic acid hybrids could be used as a structural optimization platform for the design and development of more selective and potent anticancer molecules.

Received 27th April 2019
Accepted 20th May 2019

DOI: 10.1039/c9ra03151k

rsc.li/rsc-advances

Introduction

Cancer has affected our ancestors throughout history. Today, cancer remains a major health concern worldwide, and is considered a life-threatening disease, representing the second most frequent cause of mortality after cardiovascular diseases, particularly in developed countries.

Although many advances have been made in understanding cancer biology, the ultimate goal of controlling this malignancy remains a distant possibility. Cancer cells closely resemble normal cells because they result from the uncontrolled growth of otherwise normal cells. Most currently available chemotherapeutic agents for cancer act against all rapidly proliferating cells. Therefore, their activities against carcinoma cells are nonselective, killing both cancer and some normal cells, specifically those dividing rapidly. Furthermore, potent and effective compounds developed for use as treatments are often associated with undesired toxic side effects. Therefore, strategic therapies for cancer continues to be a fascinating challenge and remain among the most urgent areas of research in medicinal chemistry.[1–3]

The exploration of new heterocyclic compounds that exhibit potency for multiple biological purposes remains an intriguing scientific effort. For instance, triazoles and their annulated heterocycles have received great interest owing to their synthetic and pharmacophore features, and potential applicability to a range of bioactivities, such as anticancer, antibacterial, antiviral, and anti-inflammation activities. Furthermore, these compounds can be attractive moieties for the combination of two pharmacophore fragments into one compound to generate innovative multifunctional molecules.[4–14]

Recently, we reported that triazoloquinazolines, which are derived from the combination of triazole and quinazoline, constitute an interesting antitumor class of compounds. For instance, 3-pyridyl-bis-[1,2,4]triazoloquinazoline and 5-ethoxytriazoloquinazoline have shown the highest cytotoxicity against Hep-G2 and colon HCT-116 carcinoma cells.[15] Furthermore, 5-chloro-[1,2,4] triazoloquinazolines have been found to possess promising anticancer activities against medulloblastoma (Daoy) and melanoma (SK-MEL28) cell lines.[16–18]

[a]Department of Pharmaceutical Chemistry, College of Pharmacy, King Saud University, PO Box 2457, Riyadh 11451, Saudi Arabia. E-mail: ralsalahi@ksu.edu.sa
[b]Department of Tanning Materials and Leather Technology, National Research Centre, 33 El-Bohouth St. (Former El-Tahrir St.), Dokki, Cairo 12622, Egypt
[c]Chemistry of Natural Products Group, Center of Excellence for Advanced Sciences, National Research Centre, 33 El-Bohouth St. (Former El-Tahrir St.), Dokki, Cairo 12622, Egypt
[d]Medicinal Aromatic, and Poisonous Plants Research Center, College of Pharmacy, King Saud University, PO Box 2457, Riyadh, 11451, Saudi Arabia
[e]Pharmacognosy Department, College of Pharmacy, King Saud University, PO Box 2457, Riyadh, 11451, Saudi Arabia
[f]Department of Chemistry, Faculty of Science and Technology, El-Neelain University, PO Box 12702, Khartoum 11121, Sudan
[g]Department of Pharmaceutical Chemistry, Drug Exploration and Development Chair (DEDC), College of Pharmacy, King Saud University, Riyadh 11451, Saudi Arabia
[h]Peptide Chemistry Department, Chemical Industries Research Division, National Research Centre, 33 El-Bohouth St. (Former El-Tahrir St.), Dokki, Cairo 12622, Egypt

† Electronic supplementary information (ESI) available. See DOI: 10.1039/c9ra03151k

Letrozole and anastrozole containing a 1,2,4-triazole ring have been approved by the FDA and used as first-line therapies for the treatment of breast cancer in postmenopausal women owing to their apparent superiority to estrogen receptor antagonists, such as tamoxifen. In aromatase inhibitors (AIs), which are responsible for inhibiting estrogen production, the triazole ring plays a pivotal role in the chelation with heme iron.[6]

Based on the above information and our interest in determining the anticancer pharmacological activities of triazole compounds, we incorporated benzoic acid and the triazole pharmacophore into one molecule to generate novel 1,2,4-triazole benzoic acid hybrid scaffolds. Herein, we aim to describe the synthesis of seventeen hybrids (**1–17**) and evaluate their *in vitro* antiproliferative activity against HCT-116 and MCF-7 human cancer cell lines, and normal human RPE-1 cells.

Results and discussion

Chemistry

Synthetic routes for the formation of 1,2,4-triazole benzoic acid hybrids (**1–17**) are shown in Scheme 1. Briefly, 4-hydrazinobenzoic acid was reacted with dialkyl-*N*-cyanoimido(dithio)carbonate to derive 1,2,4-triazole benzoic acids **1** and **2** in good yields. The structures of **1** and **2** were confirmed by their physical properties, and by NMR and MS analyses. In the target products, the presence of the benzoic acid moiety was confirmed by the two *ortho* doublets in the range of 8.20–7.60 ppm ($J \approx 8.6$ Hz) and the COOH-singlet signal at ~13.10–13.20 in the ^{1}H NMR spectra, and their five ^{13}C-resonances, especially that of the carboxyl group at ~167.0 ppm. Similarly, the $-SCH_3$ functional group of **1** was validated by its typical resonances at ~2.6 (s) and 13.9 in the ^{1}H and ^{13}C NMR spectra, respectively. Furthermore, the 1,2,4-triazolo ring was established by assigning its two intrinsic ^{13}C-signals (C-3′ and C-5′), which were highly deshielded according to the type of functional group attached in each case. The amino group protons were assigned as broad singlets ranging from 6.80 to 7.00 ppm. Treating compound **1** or **2** with the appropriate aldehydes in ethanol for 24–36 h under reflux conditions yielded targets **3–12.** Their identities were verified by the characteristic resonances of the benzylidene functional group at ~9.00–9.50 (s) and 160.0–166.0 ppm in the ^{1}H and ^{13}C NMR, respectively.

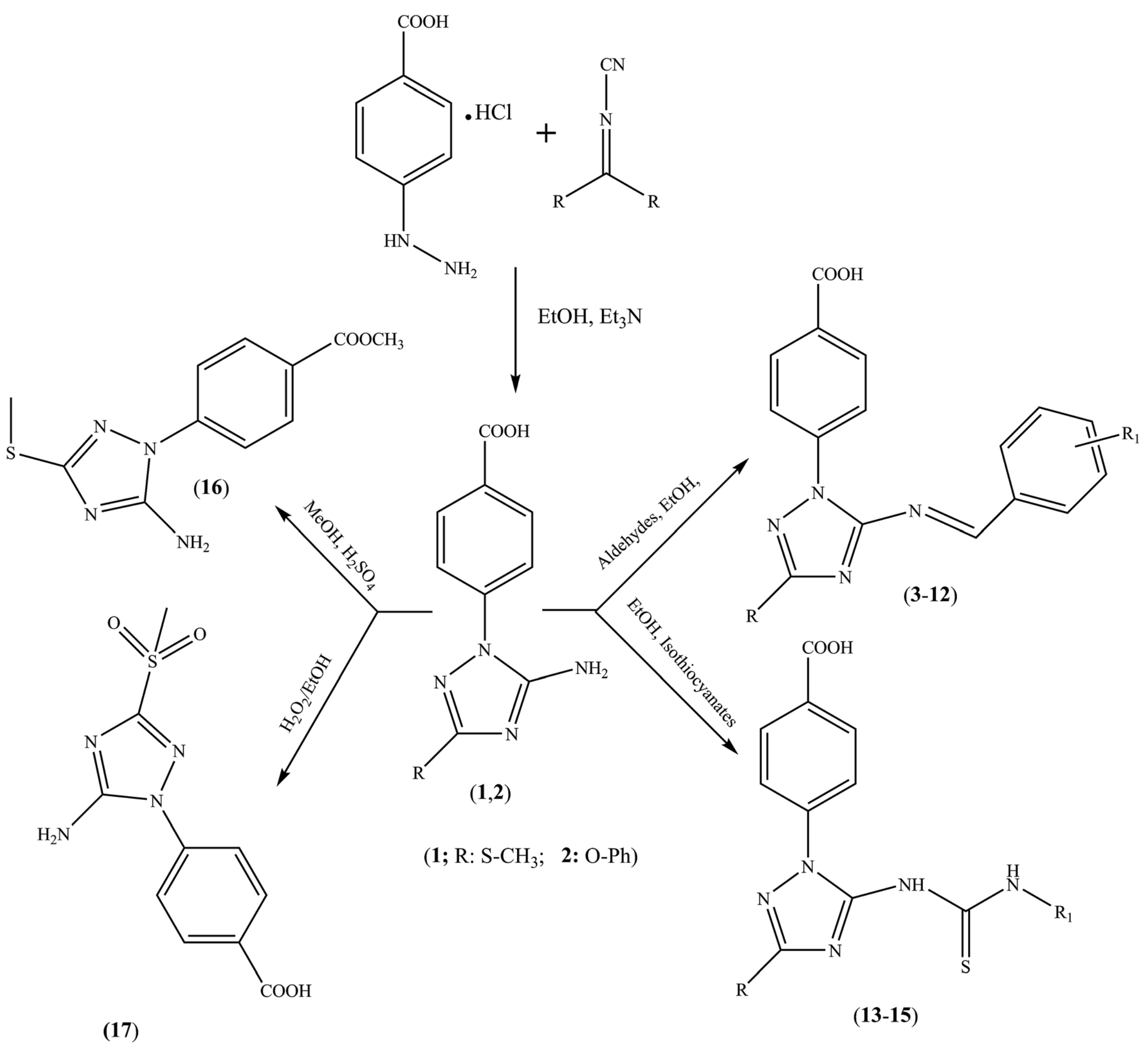

Scheme 1 Synthetic routes to triazole benzoic acid compounds 1–17.

Table 1 Synthesized triazole benzoic acid derivatives

Compound	R	R1	Compound	R	R1
3	S-CH_3	2-OH-5-methyl	**10**	O-Ph	2-OH-5-methyl
4	S-CH_3	2-OH-5-methoxy	**11**	O-Ph	2-OH-5-methoxy
5	S-CH_3	2-OH-5-nitro	**12**	O-Ph	2-OH-5-nitro
6	S-CH_3	2-OH-5-Br	**13**	S-CH_3	Benzyl
7	S-CH_3	4-OH-3-methoxy	**14**	S-CH_3	Phenethyl
8	S-CH_3	3-OH	**15**	O-Ph	Benzyl
9	S-CH_3	4-OH			

Reacting benzyl(phenethyl) isothiocyanate with parents **1** and **2** produced compounds **13–15**, whose structures were confirmed by assignment of the thiocarbonyl group peak at 188–189 ppm. Esterification of **1** yielded ester **16**, which did not have a –COOH proton signal. Furthermore, the carboxyl carbon was slightly shifted upfield (166.0 ppm) owing to ester formation, with –CH_3 resonances recorded at 3.88 and 52.8 ppm by ^{1}H and ^{13}C NMR, respectively. Oxidation of –SCH_3 to an –SO_2CH_3 group was successfully achieved by reacting **1** with hydrogen peroxide in boiling ethanol, yielding product **17**. This –SO_2CH_3 group was deduced from the singlet at 2.94 ppm in the ^{1}H NMR spectrum, and a corresponding ^{13}C resonance at 38.7 ppm. For the 3′-phenoxy products (**2**, **10–12**, and **15**), a characteristic coupling system of three ^{1}H signals was recorded at ~7.40 (br t, H-3/5), 7.27 (br d, 2/6), and 7.19 ppm (br t, H-4). Unambiguous confirmation of all products was finally achieved by clear identification of the ^{1}H and ^{13}C resonances of the accompanying functional groups or moieties, such as –SCH_3, –SO_2CH_3, –OPh, benzyl, and phenethyl, and through comparison with data of structurally related compounds.[19–24]

Biology

From the afore-mentioned synthetic routes, we obtained a series of novel 1,2,4-triazole-benzoic acid hybrids **1–17** (Table 1). To investigate whether substituents affected their cytotoxic effects, *in vitro* cytotoxic studies against HCT-116 and MCF-7 human cancer cells, and normal human RPE-1 cells, were performed using the MTT assay. Doxorubicin was used as the reference drug.

The percentages of viable cells were calculated and compared with those treated with doxorubicin. The activities of compounds **1–17** against the two cell lines were compared with those of doxorubicin. All compounds suppressed the human cell lines in a dose-dependent manner (see ESI†). To determine the efficacy of the synthesized 1,2,4-triazole benzoic acid hybrids, the cytotoxic effect of each compound was compared with that of the reference drug. Table 2 shows that compounds **2**, **5**, **12**, **14**, and **15** had significantly more potent cytotoxic activities in relation to doxorubicin against the two examined cells. The remaining compounds had significantly lower cytotoxic effects. For MCF-7 cells, **2**, **5**, **12**, **14**, and **17** exhibited the highest activities compared with that of doxorubicin. Among them, compounds **2** and **14** appeared more active than doxorubicin, while compounds **5**, **12**, **13**, **15** and **17** showed comparable activities. Compounds **1**, **3**, **4**, **6–11**, and **16** had slightly lower anticancer activities. Against HCT-116 cells, compounds **2**, **5**, **12**, **14**, and **15** were found to possess good cytotoxicity compared with doxorubicin, while the remaining compounds showed less activity. Concerning RPE-1 cells,

Table 2 Cytotoxic activity of targets **1–17** against HCT-116 and FMC-7 cancer cell lines

	IC_{50} (μM) ± SD			Therapeutic index (TI)	
Compound code	HCT-116	MCF-7	RPE-1	HCT-116	MCF-7
1	41.8 ± 6.5	32.9 ± 5.3	61.0 ± 13.9	1.5	1.9
2	25.7 ± 4.1	18.7 ± 3.5	61.2 ± 10.9	2.4	3.3
3	36.0 ± 6.1	23.9 ± 1.6	43.9 ± 10.5	1.2	1.8
4	35.2 ± 5.2	27.3 ± 4.2	55.3 ± 11.1	1.6	2.0
5	24.0 ± 4.5	20.0 ± 4.1	60.2 ± 12.8	2.5	3.0
6	37.6 ± 6.4	31.3 ± 5.1	59.4 ± 11.7	1.6	1.9
7	29.8 ± 4.2	29.4 ± 5.3	61.1 ± 12.5	2.1	2.1
8	34.6 ± 6.1	31.2 ± 5.6	70.1 ± 15.3	2.0	2.2
9	39.1 ± 5.6	34.8 ± 5.5	68.0 ± 16.7	1.7	2.0
10	33.7 ± 5.2	30.3 ± 5.3	74.0 ± 16.5	2.2	2.4
11	33.1 ± 4.4	27.5 ± 4.1	58.5 ± 10.7	1.8	2.1
12	26.8 ± 4.5	21.6 ± 3.1	62.8 ± 13.9	2.3	2.9
13	30.1 ± 4.1	23.4 ± 4.6	63.9 ± 13.5	2.1	2.7
14	28.3 ± 5.2	15.6 ± 2.2	45.8 ± 8.9	1.6	2.9
15	23.9 ± 4.5	24.0 ± 4.3	91.6 ± 15.9	3.8	3.8
16	37.3 ± 6.1	23.4 ± 3.5	39.1 ± 9.9	1.0	1.7
17	34.2 ± 5.2	21.9 ± 4.2	48.5 ± 9.8	1.4	2.2
Doxorubicin	22.6 ± 3.9	19.7 ± 3.1	64.0 ± 13.2	2.8	3.3

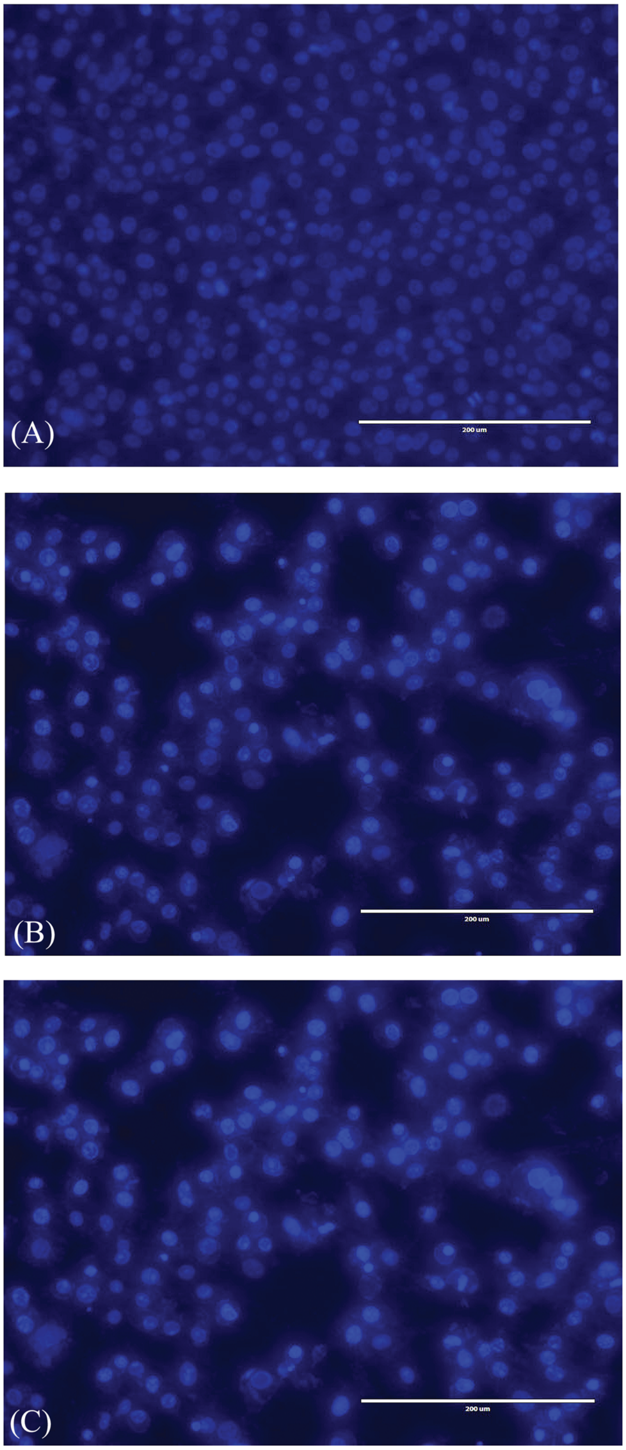

Fig. 1 Nuclear morphological changes in MCF-7 cell lines. Cells were fixed and stained with Hoechst 33258, and the images were captured by fluorescence microscopy (EVOS, USA); magnification: 200×. (A) Control (without treatment); (B and C) treatment with compounds **2** and **14** at the IC_{50} (18.7 and 15.6 μM, respectively) for 24 h. Arrows indicate apoptotic cells.

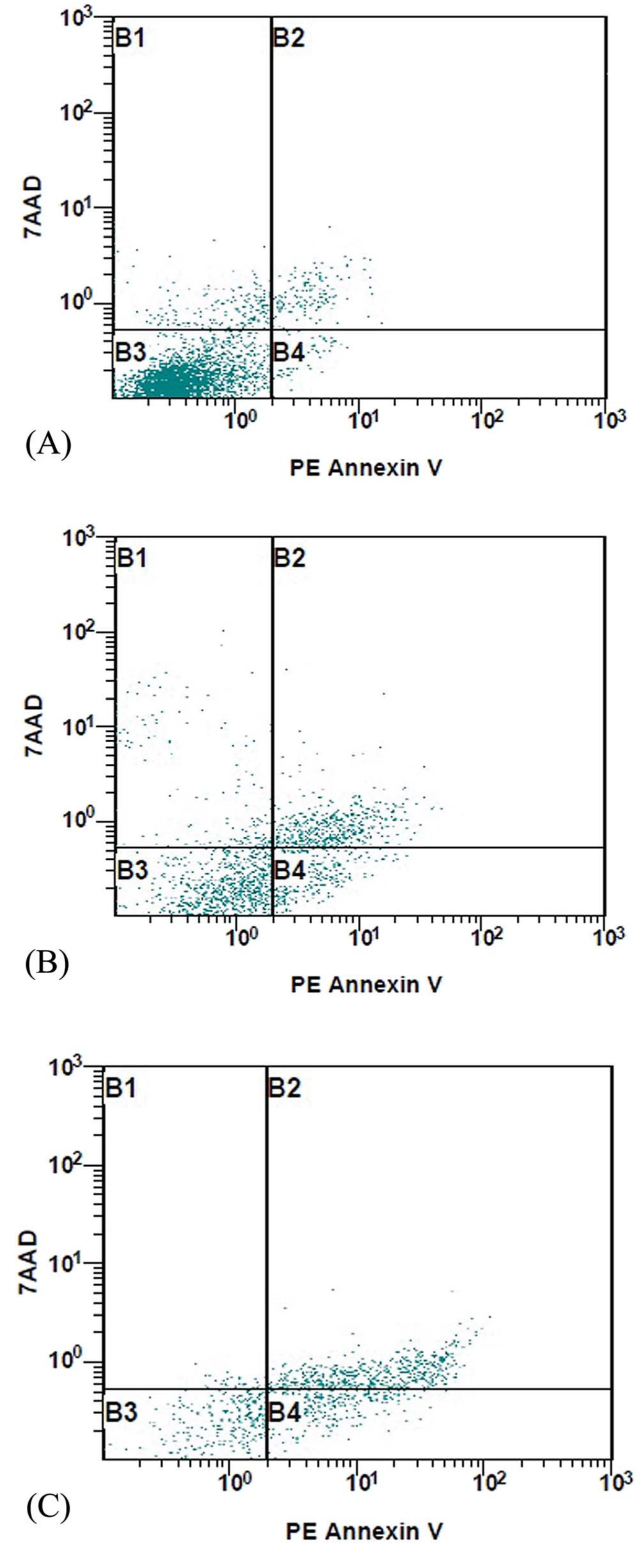

Fig. 2 Effects of compounds **2** and **14** on apoptosis induction in MCF-7 cells. MCF-7 tumor cells were grown, treated, and stained with PE Annexin V and 7-AAD dye prior to flow cytometry analysis. Lower left quadrants (B3) show live cells; lower right quadrants (B4) represent early apoptotic cells; upper left and right quadrants (B1 and B2) contain necrotic or late apoptotic cells. (A) Control (without treatment); (B and C) treatment with compounds **2** and **14** at the IC_{50} (18.7 and 15.6 μM, respectively) for 24 h.

compounds **3**, **4**, **11**, **14**, **16**, and **17** were more cytotoxic than the reference drug, while **12** and **13** had comparable effects. Furthermore, products **1**, **2**, **5**, **7**, and **9** had slightly weaker cytotoxic effects and the remaining compounds showed significantly lower cytotoxicity (Table 2 and ESI†).

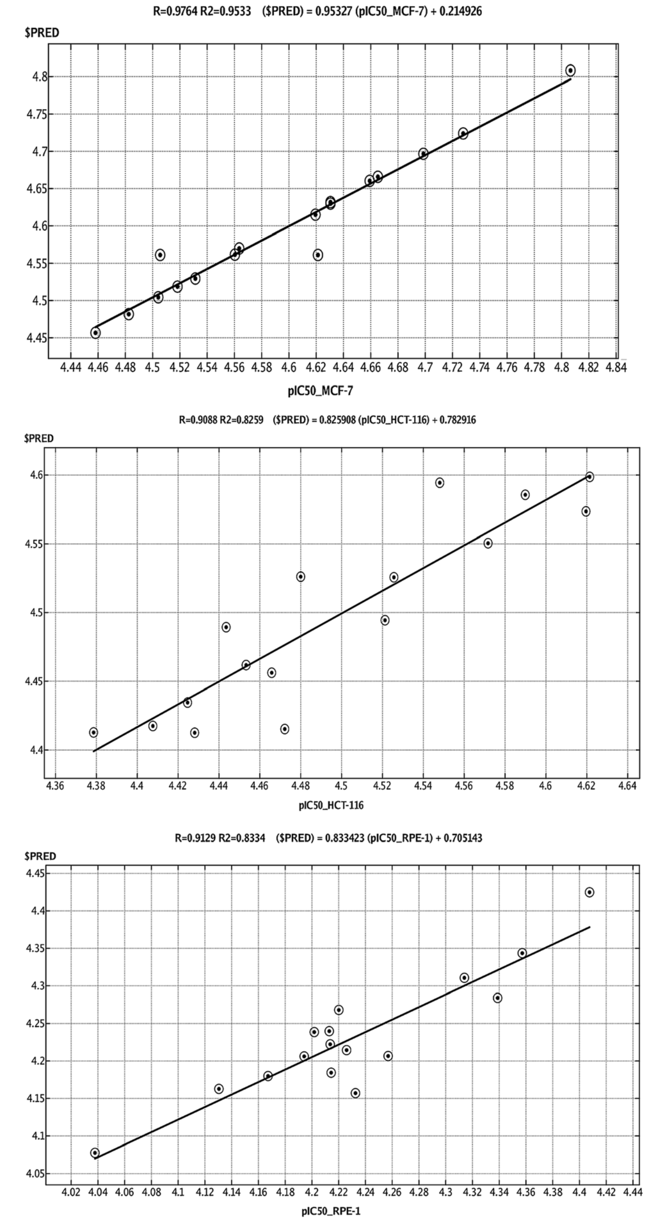

Fig. 3 Linear correlation graph of experimentally measured pIC_{50} values of compounds **1–17** against (A) breast and (B) colon cancer cell lines, and (C) RPE-1 cell lines with predicted pIC_{50} values based on the calculated 2D QSAR model. The linearity of the 2D QSAR models are shown with error (RMSE) and correlation factor (R2) values.

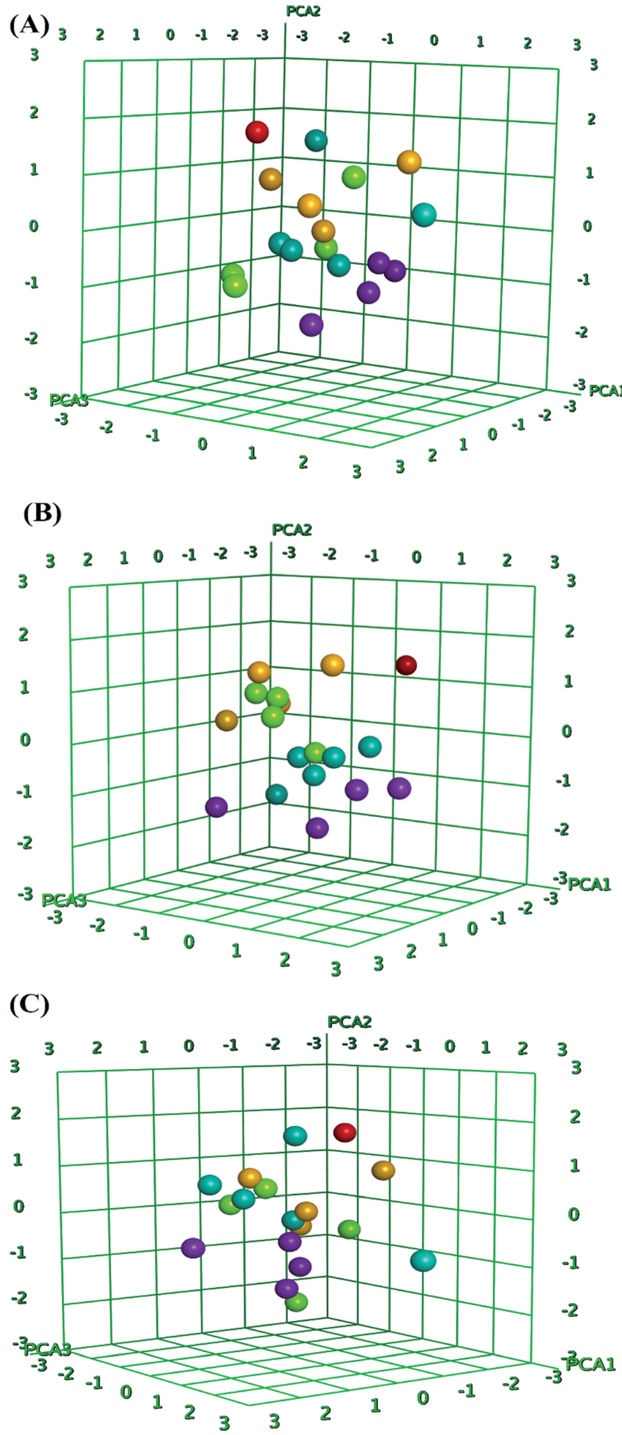

Fig. 4 Principal component analysis (PCA) plots of compounds **1–17** for data obtained for breast (A), colon cancer cells (B) and (C) RPE-1 cell line. The 3D graphical plot was constructed with three eigenvectors PCA1, PCA2 and PCA3 in the range of +3 to −3 and coordinate value for each compound has represented with colored spots.

To determine the safety of each compound, we calculated their respective therapeutic indexes (TIs) using the following equation:

$$\mathrm{TI} = \mathrm{IC}_{50} \text{ against normal cells}/\mathrm{IC}_{50} \text{ against cancer cells}$$

Table 2 shows that, for HCT-116, compound **15** had a wider TI than doxorubicin. Compounds **2**, **5**, **8**, **10**, **12**, and **13** had slightly lower TIs, while the remaining compounds had a significantly lower TI than doxorubicin.

Similarly, compared with doxorubicin, compound **15** had wider TI against MCF-7 cells, while **2** had the same TI, compounds **5** and **12–14** had slightly lower TIs, and the remaining compounds had significantly lower TIs. Regarding compound safety and efficacy, the results suggested that **2**, **5**, **14**, and **15** are potent anticancer candidate drugs in human HCT-116 and MCF-7 cancer cell lines.

The resulting findings showed that 1,2,4-triazole hybrids (**1–17**) had weak to high cytotoxic activities against the two tumor cell lines, with IC_{50} value ranges of 15.6–39.8 and 23.9–41.8 μM for MCF-7 and HCT-116 cells, respectively (Table 2). Generally, introducing an electron-rich group significantly increased the compound cytotoxicity, as exemplified by target **2**, which demonstrated promising IC_{50} values of 18.7 and 25.7 μM against MCF-7 and HCT-116, respectively.

Different substituents at the 5-position of the 1,2,4-triazole moiety in **2** contributed to the cytotoxicity profile. Furthermore, SAR studies showed that introducing isothiocyanate (**15**) and nitrobenzylidene (**12**) substituents was crucial for the potent cytotoxic activity.

Although target **1** was less active, its transformed product **5** showed the highest activity among all test compounds. Compound **7** showed a moderate effect against both cancer cell lines. Through this work, we found that aldehyde substituents at the 5-position showed varying cytotoxicities, as indicated by compounds **3–12**.

Furthermore, the selectivity of chemotherapeutic agents remains a major impediment to successful cancer therapy. Therefore, the discovery and design of new chemical entities that can exert selectivity towards carcinoma cells are likely to improve the therapeutic index.

Apoptosis detection

MCF-7 cells were treated with **2** and **14** at 18.7 and 15.6 μM, respectively, for 24 h, stained with fluorescence DNA-binding dye Hoechst 33258. As shown in (Fig. 1) DNA fragmentation and typical marks of apoptosis are evident after compounds treatment. In contrast, control or vehicle-treated cells retained their cellular morphology, confluency and uniformly stained. To further confirm the apoptosis detection, MCF-7 treated cells were analyzed by flow cytometry. This method is based on the binding of Annexin V to phosphatidylserine on the plasma membrane of cells that undergoes apoptosis. In contrast, 7-amino-actinomycin (7-AAD) bind to the nucleic acids of cells in the later stages of apoptosis or necrosis. The results indicated that **2** and **14** induced cell apoptosis in MCF-7 cells. The MCF-7 control gave apoptosis percentage of 1.84 ± 0.63 and 2.94 ± 0.5% in early and late apoptosis, respectively, while treated cells showed an increase of 17.82 ± 1.30 and 24.91 ± 1.98% with compound **2** and 29.11 ± 1.44 and 45.47 ± 2.10 % with compound **14** in early and late apoptosis, respectively. As shown in Fig. 2, there was a significant difference ($p < 0.05$) in the early and late apoptosis of the control and MCF-7 treated cells. Apparently, compound **2** and **14** can mediate apoptosis in cancer cells, which contributed, at least in part, to their cytotoxic effects.

2D QSAR analysis

QSAR is a method used to analyze the molecular descriptors (molecular weight, SlogP, HBA, HBD, rotatable bonds, and TPSA) of ligands/drugs and their correlation with *in vitro*/*in vivo* biological characteristics. The QuaSAR module was employed in the MOE to perform 2D QSAR for compounds **1–17**. The calculated pIC_{50} values for compounds **1–17** against MCF-7 and HCT-116 cancer cells were input manually. Correlation plots were generated by plotting pIC_{50} values on the *x*-axis and predicted values ($PRED) on the *y*-axis for compounds **1–17**.[6] From the resulting pIC_{50} and $PRED values, a 2D QSAR model for compounds **1–17** was created to investigate potential ligand compounds. Regression plots were built for pIC_{50} *vs.* $PRED for the two cancer cells and the normal cells. A linear correlation resulted from regression analysis of the target compounds against MCF-7 cancer cells, exhibiting excellent linearity (Fig. 3). The *Z*-score of compounds **1–17** was predicted for the two cancer cells and normal cells. All compounds, except **3** and **8**, showed good *Z*-score values. Compounds **3** and **8** showed *Z*-score values (absolute difference between the value of the model and the activity field, divided by the square root of the mean square error of the data set) beyond the limit of 2.5 (2.985 and 2.803). Compounds **2**, **5**, **14**, and **15** showed more significant *Z*-scores of 0.175, 0.0779, 0.0998, and 0.208, respectively, against the MCF-7 cells. Compound **15** had a significant *Z* score of 0.733 against HCT-116 cells. Furthermore, principal component analysis was performed using the three eigenvectors, namely, PCA1, PCA2, and PCA3, and 3D graphical plots were created that included 98% of variance. In the plot, all values were found to lie in the range of +3 to −3 and are shown as different colored spots in Fig. 4, with each colored spot representing one compound.[6]

Conclusions

A series of novel 1,2,4-triazole benzoic acid derivatives were synthesized, and their potential *in vitro* cytotoxicity against MCF-7 and HCT-116 human cancer cell lines was determined. Through this investigation, we showed that hybrids **2**, **5**, **14**, and **15** exhibited potent antiproliferative activities. The SAR study also showed that the incorporation of isothiocyanate and nitrobenzylidene moieties into the 1,2,4-triazole scaffold would be beneficial to its promising cytotoxic effects. Furthermore, **2** and **15** not only demonstrated promising cytotoxic effects against the examined tumor cells, but exhibited very weak cytotoxicity against normal cells, implying that a therapeutic window exists for their use. A confirmation test also indicated that compounds **2** and **14** induce apoptosis in MCF-7 cancer cells and are, therefore, worthy of further research to develop novel anticancer drugs. In 2D QSAR analysis, the predicted pIC_{50} values of active compounds showed significant correlations with the experimental values from the generated regression and principal component analysis plots. These results strongly support the cytotoxicity results of compounds **2**, **5**, **14**, and **15**.

Materials and methods

Chemistry

General. Melting points were uncorrected and determined with open glass capillaries using a STUART melting point SMP 10 apparatus. High-resolution mass spectra were obtained on a JEOL MStation JMS-700 system. ^{1}H and ^{13}C NMR spectra (500, 700, and 175 MHz) were recorded on Bruker AMX 500 and 700 instruments using TMS as the internal reference and DMSO-d_6 as solvent.

General procedure for the preparation of compounds 1 and 2

Through dropwise addition, 2-hydrazinobenzoic acid (10 mmol) dissolved in EtOH (10 mL) and Et_3N (20 mmol) was added to a solution of dimethyl(phenyl)-*N*-cyanoimido(dithio)carbonate at room temperature. The mixture was refluxed for 3–5 h and then poured into ice/water. The obtained solid was collected, washed with water, and dried.

4-(5-Amino-3-(methylthio)-1*H*-1,2,4-triazol-1-yl)benzoic acid (1). Pale yellow amorphous powder (70%); mp 174–176 °C (DMF); ^{1}H NMR (700 MHz, DMSO-d_6): δ 13.09 (br s, 1H, –COO<u>H</u>), 8.05 (d, $J = 8.7$ Hz, 2H, H-2/6), 7.68 (d, $J = 8.7$ Hz, 2H, H-3/5), 6.79 (br s, 2H,–N<u>H</u>$_2$), 2.49 (s, 3H, –SC<u>H</u>$_3$); ^{13}C NMR (175 MHz, DMSO-d_6): δ 167.1 (C-7), 159.3 (C-3′), 155.9 (C-5′), 140.9 (C-4), 131.1 (C-2/6), 128.8 (C-1), 121.9 (C-3/5), 13.8 (–S<u>C</u>H$_3$); HRMS (EI): *m*/*z* calcd for $C_{10}H_{10}N_4O_2S$ $(M)^{\cdot+}$ 250.0524, found 250.0563.

4-(5-Amino-3-phenoxy-1*H*-1,2,4-triazol-1-yl)benzoic acid (2). Pale yellow amorphous powder (73%); mp 240–242 °C; ^{1}H NMR (700 MHz, DMSO-d_6): δ 13.09 (br s, 1H, –COO<u>H</u>), 8.04 (d, $J =$ 8.6 Hz, 2H, H-2/6), 7.66 (d, $J = 8.6$ Hz, 2H, H-3/5), 7.41 (br t, $J =$ 7.5 Hz, 2H, H-3′/5′), 7.27 (br d, $J = 7.8$ Hz, 2H, H-2′/6′), 7.19 (br t, $J = 7.5$ Hz, 1H, H-4′), 6.92 (br s, 2H, –N<u>H</u>$_2$); ^{13}C NMR (175 MHz, DMSO-d_6): δ 167.1 (C-7), 164.8 (C-3′), 155.0 (C-5′), 154.9 (C-1″), 140.9 (C-4), 131.1 (C-2/6), 130.1 (C-3″/5″ & 1), 124.8 (C-4″), 121.9 (C-3/5), 119.8 (C-2″/6″); HRMS (EI): *m*/*z* calcd for $C_{15}H_{12}N_4O_3$ $(M)^{\cdot+}$ 296.0909, found 296.0947.

General procedure for the preparation of compounds 3–15

A mixture of aldehyde (1.1 mmol) or benzyl (phenethyl)isothiocyanate (1.1 mmol) with compounds **1** and **2** (1 mmol) was heated under reflux in ethanol (15 mL) for 24–36 h. After cooling, the precipitate was collected by filtration, washed with water, and dried.

(*E*)-4-(5-((2-Hydroxy-5-methylbenzylidene)amino)-3-(methylthio)-1*H*-1,2,4-triazol-1-yl)benzoic acid (3). Yellow amorphous powder; yield (60%); mp 294–296 °C; ^{1}H NMR (700 MHz, DMSO-d_6): δ 13.22 (br s, 1H, –COO<u>H</u>), 10.94 (br s, 1H, –O<u>H</u>), 9.51 (s, 1H, H-7″), 8.13 (d, $J = 8.6$ Hz, 2H, H-2/6), 7.95 (d, $J = 8.6$ Hz, 2H, H-3/5), 7.71 (d, $J = 1.3$ Hz, 1H, H-6″), 7.33 (dd, $J = 8.4$, 1.3 Hz, 1H, H-4″), 6.91 (d, $J = 8.4$ Hz, 1H, H-3″), 2.63 (s, 3H, –SC<u>H</u>$_3$), 2.27 (s, 3H, –ArC<u>H</u>$_3$); ^{13}C NMR (175 MHz, DMSO-d_6): δ 167.0 (C-7), 166.1 (C-7″), 160.9 (C-3′), 159.0 (C-2″), 157.7 (C-5′), 140.3 (C-4), 137.2 (C-4″), 130.9 (C-2/6), 130.2 (C-5″), 130.1 (C-6″), 129.0 (C-1), 123.5 (C-3/5), 120.2 (C-1″), 117.3 (C-3″), 20.4 (–Ar<u>C</u>H$_3$), 13.9 (–S<u>C</u>H$_3$); HRMS (EI): *m*/*z* calcd for $C_{18}H_{16}N_4O_3S$ $(M)^{\cdot+}$ 368.0943, found 368.0980.

(*E*)-4-(5-((2-Hydroxy-5-methoxybenzylidene)amino)-3-(methylthio)-1*H*-1,2,4-triazol-1-yl)benzoic acid (4). Pale yellow amorphous powder (63%); mp 278–280 °C; ^{1}H NMR (700 MHz, DMSO-d_6): δ 13.21 (br s, 1H, –COO<u>H</u>), 10.72 (br s, 1H, –O<u>H</u>), 9.52 (s, 1H, H-7″), 8.12 (d, $J = 8.4$ Hz, 2H, H-2/6), 7.97 (d, $J = 8.4$ Hz, 2H, H-3/5), 7.44 (d, $J = 2.8$ Hz, 1H, H-6″), 7.15 (dd, $J = 8.9$, 2.8 Hz, 1H, H-4″), 6.95 (d, $J = 8.9$ Hz, 1H, H-3″), 3.75 (s, 3H, –OC<u>H</u>$_3$), 2.64 (s, 3H, –SC<u>H</u>$_3$); ^{13}C NMR (175 MHz, DMSO-d_6): δ 167.0 (C-7), 165.5 (C-7″), 161.0 (C-3′), 157.6 (C-5′), 155.5 (C-2″), 152.7 (C-5″), 140.3 (C-4), 130.8 (C-2/6), 130.2 (C-1), 124.2 (C-4″), 123.5 (C-3/5), 120.5 (C-1″), 118.6 (C-3″), 111.8 (C-6″), 55.9 (–O<u>C</u>H$_3$), 13.9 (–S<u>C</u>H$_3$); HRMS (EI): *m*/*z* calcd for $C_{18}H_{16}N_4O_4S$ $(M)^{\cdot+}$ 384.0892, found 384.0912.

(*E*)-4-(5-((2-Hydroxy-5-nitrobenzylidene)amino)-3-(methylthio)-1*H*-1,2,4-triazol-1-yl)benzoic acid (5). Yellow amorphous powder; yield (61%); mp > 300 °C; ^{1}H NMR (700 MHz, DMSO-d_6): δ 13.13 (br s, 1H, –COO<u>H</u>), 10.31 (br s, 1H, –O<u>H</u>), 9.55 (s, 1H, H-7″), 8.75 (d, $J = 2.6$ Hz, 1H, H-6″), 8.37 (dd, $J = 9.1$, 2.6 Hz, 1H, H-4″), 8.05 (d, $J = 8.5$ Hz, 2H, H-2/6), 7.68 (d, $J = 8.4$ Hz, 2H, H-3/5), 7.19 (d, $J = 9.1$ Hz, 1H, H-3″), 2.65 (s, 3H, –SC<u>H</u>$_3$); ^{13}C NMR (175 MHz, DMSO-d_6): δ 167.1 (C-7), 166.1 (C-7″), 161.2 (C-3′), 157.7 (C-5′), 156.0 (C-2″), 140.5 (C-4), 140.2 (C-5″), 131.1 (C-2/6), 130.5 (C-1), 122.7 (C-4″), 121.9 (C-3/5), 121.5 (C-1″), 118.9 (C-3″), 118.3 (C-6″), 13.8 (–S<u>C</u>H$_3$); HRMS (EI): *m*/*z* calcd for $C_{17}H_{13}N_5O_5S$ $(M)^{\cdot+}$ 399.0637, found 399.0686.

(*E*)-4-(5-((5-Bromo-2-hydroxybenzylidene)amino)-3-(methylthio)-1*H*-1,2,4-triazol-1-yl)benzoic acid (6). Yellow amorphous powder; yield (58%); mp > 300 °C; ^{1}H NMR (700 MHz, DMSO-d_6): δ 13.20 (br s, 1H, –COO<u>H</u>), 10.22 (br s, 1H, –O<u>H</u>), 9.49 (s, 1H, H-7″), 8.12 (d, $J = 8.6$ Hz, 2H, H-2/6), 7.93 (d, $J = 8.6$ Hz, 2H, H-3/5), 7.72 (d, $J = 2.6$ Hz, 1H, H-6″), 7.49 (dd, $J = 8.4$, 2.6 Hz, 1H, H-4″), 6.95 (d, $J = 8.4$ Hz, 1H, H-3″), 2.64 (s, 3H, –SC<u>H</u>$_3$); ^{13}C NMR (175 MHz, DMSO-d_6): δ 167.0 (C-7), 164.2 (C-7″), 161.1 (C-3′), 159.9 (C-2″), 157.4 (C-5′), 140.1 (C-4), 134.6 (C-4″), 131.1 (C-6″), 130.8 (C-2/6), 130.3 (C-1), 123.7 (C-3/5), 122.0 (C-1″), 119.2 (C-3″), 111.2 (C-5″), 13.9 (–S<u>C</u>H$_3$); HRMS (EI): *m*/*z* calcd for $C_{17}H_{13}BrN_4O_3S$ $(M)^{\cdot+}$431.9892, found 431.9924.

(*E*)-4-(5-((4-Hydroxy-3-methoxybenzylidene)amino)-3-(methylthio)-1*H*-1,2,4-triazol-1-yl)benzoic acid (7). Pale yellow amorphous powder; yield (50%); mp 213–215 °C, (DMF); ^{1}H NMR (700 MHz, DMSO-d_6): δ 13.12 (br s, 1H, –COO<u>H</u>), 9.77 (br s, 1H, –O<u>H</u>), 9.17 (s, 1H, H-7″), 8.13 (d, $J = 8.7$ Hz, 2H, H-2/6), 8.04 (d, $J = 8.7$ Hz, 2H, H-3/5), 7.63 (d, $J = 1.8$ Hz, 1H, H-2″), 7.60 (dd, $J =$ 8.1, 1.8 Hz, 1H, H-6″), 6.97 (d, $J = 8.1$ Hz, 1H, H-5″), 3.87 (s, 3H, –OC<u>H</u>$_3$), 2.63 (s, 3H, –SC<u>H</u>$_3$); ^{13}C NMR (175 MHz, DMSO-d_6): δ 167.8 (C-7), 160.7 (C-7″), 159.3 (C-3′), 155.9 (C-5′), 153.3 (C-4″), 148.6 (C-3″), 140.6 (C-4), 131.1 (C-2/6), 129.6 (C-1″), 129.2 (C-1), 126.7 (C-6″), 122.8 (C-3/5), 113.1 (C-2″), 56.0 (–O<u>C</u>H$_3$), 13.9 (–S<u>C</u>H$_3$); HRMS (EI): *m*/*z* calcd for $C_{18}H_{16}N_4O_4S$ $(M)^{\cdot+}$ 384.0892, found 384.0923.

(*E*)-4-(5-((3-Hydroxybenzylidene)amino)-3-(methylthio)-1*H*-1,2,4-triazol-1-yl)benzoic acid (8). Pale yellow amorphous powder (59%); mp 230–232 °C; ^{1}H NMR (700 MHz, DMSO-d_6): δ 13.14 (br s, 1H, –COO<u>H</u>), 9.92 (br s, 1H, –O<u>H</u>), 9.24 (s, 1H, H-7″), 8.14 (d, $J = 8.3$ Hz, 2H, H-2/6), 7.99 (d, $J = 8.3$ Hz, 2H, H-3/5), 7.51 (br d, $J = 7.5$ Hz, 1H, H-6″), 7.47 (br s, 1H, H-2″), 7.40 (t-like, $J = 7.9$ Hz, 1H, H-5″), 7.21 (br d, $J = 7.5$ Hz, 1H, H-4″), 2.65 (s, 3H, –SC<u>H</u>$_3$); ^{13}C NMR (175 MHz, DMSO-d_6): δ 167.1 (C-7), 160.9 (C-7″), 159.3 (C-3′), 158.3 (C-3″), 155.9 (C-5′), 140.9 (C-4), 136.3 (C-1″), 130.8 (C-2/6), 130.0 (C-1), 123.4 (C-3/5), 122.9 (C-6″), 121.6 (C-4″), 115.4 (C-2″), 13.8 (–S<u>C</u>H$_3$); HRMS (EI): *m*/*z* calcd for $C_{17}H_{14}N_4O_3S$ $(M)^{\cdot+}$ 354.0787, found 354.0819.

(*E*)-4-(5-((4-Hydroxybenzylidene)amino)-3-(methylthio)-1*H*-1,2,4-triazol-1-yl)benzoic acid (9). Pale yellow amorphous powder (60%); mp 247–249 °C (DMF); ^{1}H NMR (700 MHz, DMSO-d_6): δ 13.13 (br s, 1H, –COOH), 9.19 (s, 1H, H-7″), 8.13 (d, J = 8.6 Hz, 2H, H-2/6), 8.03 (d, J = 8.6 Hz, 2H, H-3/5), 7.67 (d, J = 8.5 Hz, 2H, H-2″/6″), 6.95 (d, J = 8.5 Hz, 2H, H-3″/5″), 2.63 (s, 3H, –SCH$_3$); ^{13}C NMR (175 MHz, DMSO-d_6): δ 167.8 (C-7), 163.5 (C-4″), 160.7 (C-7″), 159.3 (C-3′), 155.9 (C-5′), 140.9 (C-4), 133.4 (C-1″), 131.1 (C-2/6), 130.8 (C-2″/6″), 129.7 (C-1), 122.9 (C-3/5), 116.7 (C-3″/5″), 13.9 (–SCH$_3$); HRMS (EI): m/z calcd for $C_{17}H_{14}N_4O_3S$ $(M)^{\bullet+}$ 354.0787, found 354.0819.

(*E*)-4-(5-((2-Hydroxy-5-methylbenzylidene)amino)-3-phenoxy-1*H*-1,2,4-triazol-1-yl)benzoic acid (10). Pale yellow amorphous powder; yield (58%); mp 240–242 °C; ^{1}H NMR (700 MHz, DMSO-d_6): δ 13.09 (br s, 1H, –COOH), 10.23 (br s, 1H, –OH), 9.42 (s, 1H, H-7″), 8.12 (d, J = 8.6 Hz, 2H, H-2/6), 7.96 (d, J = 8.6 Hz, 2H, H-3/5), 7.72 (br s, 1H, H-6‴), 7.40 (br t, J = 7.4 Hz, 2H, H-3″/5″), 7.34 (br d, J = 8.4 Hz, 1H, H-4‴), 7.26 (br d, J = 7.8 Hz, 2H, H-2″/6″), 7.19 (br t, J = 7.5 Hz, 1H, H-4″), 6.91 (d, J = 8.4 Hz, 1H, H-3‴), 2.25 (s, 3H, –ArCH$_3$); ^{13}C NMR (175 MHz, DMSO-d_6): δ 167.1 (C-7), 166.9 (C-7‴), 164.8 (C-3′), 159.2 (C-2‴), 154.9 (C-5′/1″), 141.0 (C-4), 137.7 (C-4‴), 131.1 (C-2/6), 130.3 (C-5‴), 130.1 (C-3″/5″), 129.2 (C-1), 128.7 (C-6‴), 124.8 (C-4″), 121.9 (C-3/5), 119.8 (C-2″/6″), 119.7 (C-1‴), 117.3 (C-3‴), 20.3 (–ArCH$_3$); HRMS (EI): m/z calcd for $C_{23}H_{18}N_4O_4$ $(M)^{\bullet+}$ 414.1328, found 414.1357.

(*E*)-4-(5-((2-Hydroxy-5-methoxybenzylidene)amino)-3-phenoxy-1*H*-1,2,4-triazol-1-yl)benzoic acid (11). Pale yellow amorphous powder; yield (61%); mp 220–222 °C; ^{1}H NMR (700 MHz, DMSO-d_6): δ 13.11 (br s, 1H, –COOH), 10.26 (br s, 1H, –OH), 9.42 (s, 1H, H-7‴), 8.13 (d, J = 8.4 Hz, 2H, H-2/6), 7.96 (d, J = 8.4 Hz, 2H, H-3/5), 7.43 (br s, 1H, H-6‴), 7.41 (br t, J = 7.6 Hz, 2H, H-3″/5″), 7.26 (br d, J = 7.7 Hz, 2H, H-2″/6″), 7.15 (br d, 1H, H-4‴), 7.19 (br t, J = 7.3 Hz, 1H, H-4″), 6.95 (d, J = 8.8 Hz, 1H, H-3‴), 3.73 (s, 3H, –OCH$_3$); ^{13}C NMR (175 MHz, DMSO-d_6): δ 167.1 (C-7), 164.8 (C-7‴), 161.0 (C-3′), 155.8 (C-2‴), 154.9 (C-5′/1″), 152.6 (C-5‴), 141.0 (C-4), 131.1 (C-2/6), 130.1 (C-3″/5″), 128.7 (C-1), 124.8 (C-4″/4‴), 121.9 (C-3/5), 119.8 (C-2″/6″), 119.7 (C-1‴), 119.1 (C-3‴), 110.5 (C-6‴), 55.9 (–OCH$_3$); HRMS (EI): m/z calcd for $C_{23}H_{18}N_4O_5$ $(M)^{\bullet+}$ 430.1277, found 430.1304.

(*E*)-4-(5-((2-Hydroxy-5-nitrobenzylidene)amino)-3-phenoxy-1*H*-1,2,4-triazol-1-yl)benzoic acid (12). White amorphous powder; yield (60%); mp 269–271 °C; ^{1}H NMR (700 MHz, DMSO-d_6): δ 13.13 (br s, 1H, –COOH), 10.31 (br s, 1H, –OH), 9.55 (s, 1H, H-7‴), 8.75 (d, J = 2.6 Hz, 1H, H-6‴), 8.37 (dd, J = 9.1, 2.6 Hz, 1H, H-4‴), 8.05 (d, J = 8.5 Hz, 2H, H-2/6), 7.68 (d, J = 8.4 Hz, 2H, H-3/5), 7.41 (br t, J = 7.6 Hz, 2H, H-3″/5″), 7.26 (br d, J = 7.7 Hz, 2H, H-2″/6″), 7.19 (br t, J = 7.3 Hz, 1H, H-4″), 7.19 (d, J = 9.1 Hz, 1H, H-3‴); ^{13}C NMR (175 MHz, DMSO-d_6): δ 167.1 (C-7), 166.1 (C-7‴), 161.2 (C-3′), 157.7 (C-5′), 156.0 (C-2‴), 154.9 (C-1″), 140.5 (C-4), 140.2 (C-5‴), 131.1 (C-2/6), 130.1 (C-3″/5″), 130.5 (C-1), 124.8 (C-4″), 122.7 (C-4‴), 121.9 (C-3/5), 121.5 (C-1‴), 119.8 (C-2″/6″), 118.9 (C-3‴), 118.3 (C-6‴); HRMS (EI): m/z calcd for $C_{22}H_{15}N_5O_6$ $(M)^{\bullet+}$ 445.1022, found 445.1059.

4-(3-(Methylthio)-5-(3-benzylylthioureido)-1*H*-1,2,4-triazol-1-yl)benzoic acid (13). White amorphous powder; yield (48%); mp 238–240 °C; ^{1}H NMR (700 MHz, DMSO-d_6): δ 13.11 (br s, 1H, –COOH), 9.63 (br s, 1H, –NH–), 8.05 (d, J = 8.6 Hz, 2H, H-2/6), 7.68 (d, J = 8.6 Hz, 2H, H-3/5), 7.33 (br t, J = 7.5 Hz, 2H, H-3″/5″), 7.28 (br d, J = 7.3 Hz, 2H, H-2″/6″), 7.24 (br t, J = 7.5 Hz, 1H, H-4″), 4.95 (s, 2H, H-7″), 2.49 (s, 3H, –SCH$_3$); ^{13}C NMR (175 MHz, DMSO-d_6): δ 188.2 (>C=S), 167.1 (C-7), 159.4 (C-3′), 155.9 (C-5′), 140.9 (C-4), 138.6 (C-1″), 131.1 (C-2/6), 129.3 (C-3″/5″), 128.7 (C-2″/6″), 128.6 (C-1), 127.8 (C-4″), 121.9 (C-3/5), 48.5 (C-7″), 13.9 (–SCH$_3$); HRMS (EI): m/z calcd for $C_{18}H_{17}N_5O_2S_2$ $(M)^{\bullet+}$ 399.0824, found 399.0857.

4-(3-(Methylthio)-5-(3-phenethylthioureido)-1*H*-1,2,4-triazol-1-yl)benzoic acid (14). White amorphous powder; yield (51%); mp 253–255 °C; ^{1}H NMR (700 MHz, DMSO-d_6): δ 13.11 (br s, 1H, –COOH), 8.05 (d, J = 8.5 Hz, 2H, H-2/6), 7.68 (d, J = 8.6 Hz, 2H, H-3/5), 7.34 (br t, J = 7.5 Hz, 2H, H-3″/5″), 7.29 (br d, J = 7.3 Hz, 2H, H-2″/6″), 7.27 (br t, J = 7.5 Hz, 1H, H-4″), 3.92 (t, J = 6.9 Hz, 2H, H-8″), 2.96 (t, J = 6.9 Hz, 2H, H-7″), 2.49 (s, 3H, –SCH$_3$); ^{13}C NMR (175 MHz, DMSO-d_6): δ 189.9 (>C=S), 167.8 (C-7), 159.4 (C-3′), 155.9 (C-5′), 140.9 (C-4), 138.1 (C-1″), 131.1 (C-2/6), 129.4 (C-3″/5″), 128.9 (C-2″/6″), 128.8 (C-1), 127.3 (C-4″), 122.0 (C-3/5), 46.4 (C-8″), 35.8 (C-7″), 13.8 (–SCH$_3$); HRMS (EI): m/z calcd for $C_{19}H_{19}N_5O_2S_2$ $(M)^{\bullet+}$ 413.0980, found 413.1028.

4-(5-(3-Benzylylthioureido)(3-phenoxy)-1*H*-1,2,4-triazol-1-yl)benzoic acid (15). White amorphous powder; yield (58%); mp 266–268 °C; ^{1}H NMR (700 MHz, DMSO-d_6): δ 13.09 (br s, 1H, –COOH), 9.64 (br s, 1H, –NH–), 8.03 (d, J = 7.9 Hz, 2H, H-2/6), 7.66 (d, J = 7.9 Hz, 2H, H-3/5), 7.41 (br t, J = 7.6 Hz, 2H, H-3″/5″), 7.34 (br t, J = 7.5 Hz, 2H, H-3‴/5‴), 7.29 (br d, J = 7.5 Hz, 2H, H-2‴/6‴), 7.26 (m, 3H, H-2″/6″,4‴), 7.18 (br t, J = 7.7 Hz, 1H, H-4″), 4.95 (s, 2H, H-7‴); ^{13}C NMR (175 MHz, DMSO-d_6): δ 188.0 (>C=S), 167.1 (C-7), 164.8 (C-3′), 154.9 (C-5′,1″), 141.0 (C-4), 138.5 (C-1‴), 131.1 (C-2/6), 130.1 (C-3″/5″), 129.4 (C-3‴/5‴), 128.7 (C-1), 128.6 (C-2‴/6‴), 127.8 (C-4‴), 124.8 (C-4″), 121.9 (C-3/5), 119.8 (C-2″/6″), 48.5 (C-7‴); HRMS (EI): m/z calcd for $C_{23}H_{19}N_5O_3S$ $(M)^{\bullet+}$ 445.1209, found 445.1243.

General procedure for the preparation of methyl 4-(5-amino-3-(methylthio)-1*H*-1,2,4-triazol-1-yl)benzoate (16)

A mixture of compound **1** (1 mmol), methanol (10 mL), and concentrated H_2SO_4 (0.4 mL) was heated under reflux for 5 h. The mixture was then cooled to room temperature, concentrated under reduced pressure, and treated with equal volumes (20 mL) of water and CH_2Cl_2. The aqueous phase was further extracted with CH_2Cl_2, which was combined with the previous CH_2Cl_2 layer. The organic phase was washed with aqueous Na_2CO_3 (20 mL) and water (20 mL), dried over Na_2SO_4, and evaporated to obtain **16** as a pale yellow amorphous powder. Yield (42%); mp 150–152 °C; ^{1}H NMR (700 MHz, DMSO-d_6): δ 8.06 (d, J = 8.7 Hz, 2H, H-2/6), 7.71 (d, J = 8.7 Hz, 2H, H-3/5), 6.82 (br s, 2H, –NH$_2$), 3.88 (s, 3H, –CO–OCH$_3$), 2.49 (s, 3H, –SCH$_3$); ^{13}C NMR (175 MHz, DMSO-d_6): δ 166.0 (C-7), 159.5 (C-3′), 155.9 (C-5′), 141.3 (C-4), 130.9 (C-2/6), 127.5 (C-1), 121.9 (C-3/5), 52.8 (–CO–OCH$_3$), 13.8 (–SCH$_3$); HRMS (EI): m/z calcd for $C_{11}H_{12}N_4O_2S$ $(M)^{\bullet+}$ 264.0681, found 264.0727.

General procedure for the preparation of 4-(5-amino-3-(methylsulfonyl)-1*H*-1,2,4-triazol-1-yl) benzoic acid (17)

Compound **1** (1 mmol) was dissolved in boiling ethanol (10 mL). H_2O_2 (2 mL) was then added dropwise over 5 min, followed by further heating of the mixture for 3 h. The solvent was evaporated, and the remaining residue was treated with hot water and left to stand at room temperature. The resulting solid was filtered, washed with water, and dried.

White amorphous powder, yield (69%); mp 249–251 °C; ^{1}H NMR (700 MHz, DMSO-d_6): δ 13.11 (br s, 1H, –COO$\underline{H}$), 8.11 (d, J = 8.5 Hz, 2H, H-2/6), 7.72 (d, J = 8.5 Hz, 2H, H-3/5), 7.12 (br s, 2H, –N$\underline{H}_2$), 2.94 (s, 3H, –$SO_2C\underline{H}_3$); ^{13}C NMR (175 MHz, DMSO-d_6): δ 167.0 (C-7), 164.1 (C-3′), 156.6 (C-5′), 140.3 (C-4), 131.2 (C-2/6), 130.2 (C-1), 123.3 (C-3/5), 38.7 (–$SO_2\underline{C}H_3$); HRMS (EI): m/z calcd for $C_{10}H_{10}N_4O_4S$ $(M)^{\cdot+}$ 282.0432, found 282.0472.

Biology

***In vitro* cytotoxic activity.** HCT-116 (human colorectal carcinoma), MCF-7 (human breast adenocarcinoma), and RPE-1 (human normal Retina pigmented epithelium) cell cultures were purchased from the American Type Culture Collection (Rockville, MD, USA) and maintained in DMEM supplemented with 10% heat-inactivated fetal bovine serum (FBS), 100 U mL^{-1} penicillin, and 100 U mL^{-1} streptomycin. The cells were grown at 37 °C in a 5% CO_2 humidified atmosphere.

MTT cytotoxicity assay. The cytotoxic activity of the compounds against HCT-116 and MCF-7 human cancer cell lines, as well as normal RPE-1 human cells, was estimated using the 3-(4,5-dimethyl-2-thiazolyl)-2,5-diphenyl-2*H*-tetrazolium bromide (MTT) assay, which is based on reduction of the tetrazolium salt by mitochondrial dehydrogenases in viable cells.[25–27] Cells were dispensed in a 96-well sterile microplate (5 × 10^4 cells per well), and incubated at 37 °C with different concentrations of each test compound (3.125, 6.25, 12.5, and 25 μM) in DMSO or doxorubicin (positive control) for 48 h in a serum-free medium prior to the MTT assay. After incubation, the media were carefully removed and MTT (40 μL, 2.5 mg mL^{-1}) was added to each well prior to incubation for an additional 4 h. Purple formazan dye crystals were solubilized by the adding DMSO (200 μL). The absorbance was measured at 570 nm using a Spectra Max Paradigm Multi-Mode microplate reader. The relative cell viability was expressed as the mean percentage of viable cells compared with untreated control cells. All experiments were conducted in triplicate and repeats were performed on three different days. All values are shown as means ± SD. IC_{50} values were determined by a probit analysis in SPSS (IBM Corp., Armonk, NY, USA).

Apoptosis detection using fluorescent Hoechst 33258 staining. To detect the nuclear morphological characteristics of apoptosis, Hoechst 33258 (Sigma-Aldrich, US) staining was utilized. Briefly, MCF-7 cells were cultured in 12-well plates (5 × 10^4 cells per well) in the presence and absence of compounds **2** and **14** at IC_{50} concentrations of 18.7 and 15.6 μM, respectively, for 24 h, then washed twice with PBS, fixed with 4% paraformaldehyde, and permeabilized using cold methanol. Hoechst 33258 (final concentration, 0.5 μg mL^{-1}) staining was performed in the dark for 30 min. Thereafter, cells were examined for nuclear changes (chromatin condensation and nuclear fragmentation) using fluorescence microscopy (EVOS, US).

Apoptosis quantification using flow cytometry. To determine the effects of these compounds on apoptosis induction, flow cytometry quantification of apoptotic cells was performed using a PE Annexin V Apoptosis Detection Kit with 7-AAD according to manufacturer instructions (Biolegend, CA, USA). Briefly, MCF-7 cells (5 × 10^4 cells per well) were cultured in 12-well plates. After 24 h, the cells were treated with an IC_{50} of 18.7 and 15.6 μM, respectively, and incubated for 24 h. Following incubation, cells were washed twice with cold PBS, resuspended in Annexin V binding buffer, and incubated with Annexin V-PE (5 μL) and 7-AAD (5 μL) for 15 min in the dark at room temperature. The cells were then analyzed by flow cytometry (Beckman coulter, CA, USA). Each sample was tested in triplicate.[28,29]

2D QSAR analysis. Detailed methodology has been reported in the literature (see ESI†).[6]

Conflicts of interest

The authors declare that they have no competing interests.

Note added after first publication

This article replaces the version published on 17 Jun 2019, which contained errors in Fig. 4. The correct version of this figure is now shown.

Acknowledgements

The authors wish to thank the Deanship of Scientific Research at King Saud University for funding this work through the research group No. RG-1435-068.

References

1 R. Al-Salahi, I. Alswaidan and M. Marzouk, *Int. J. Mol. Sci.*, 2014, **15**, 22483–22491.
2 H. A. Abuelizz, M. Marzouk, H. Ghabbour and R. Al-Salahi, *Saudi Pharm. J.*, 2017, **25**, 1047–1054.
3 R. Al-Salahi, R. A. El Dib and M. Marzouk, *Heterocycles*, 2015, **91**, 1735–1751.
4 H. A. M. El-Sherief, B. G. M. Youssif, S. N. Abbas-Bukhari, A. H. Abdelazeem, M. Abdel-Aziz and H. M. Abdel-Rahman, *Eur. J. Med. Chem.*, 2018, **156**, 774–789.
5 R. R. Ruddarraju, A. C. Murugulla, R. Kotla, T. M. Chandra Babu, R. Wudayagiri, S. Donthabakthuni, R. Maroju, K. Baburao and L. S. Parasa, *Eur. J. Med. Chem.*, 2016, **123**, 379–396.
6 R. Pingaew, V. Prachayasittikul, P. Mandi, C. Nantasenamat, S. Prachayasittikul, S. Ruchirawat and V. Prachayasittikul, *Bioorg. Med. Chem.*, 2015, **23**, 3472–3480.
7 W. Hou, Z. Luo, G. Zhang, D. Cao, D. Li, H. Ruan, B. H. Ruan, L. Su and H. Xu, *Eur. J. Med. Chem.*, 2017, **138**, 1042–1052.
8 T. G. Kraljević, A. Harej, M. Sedić, S. K. Pavelić, V. Stepanić, D. Drenjančević, J. Talapko and S. Raić-Malić, *Eur. J. Med. Chem.*, 2016, **124**, 794–808.
9 M. Huang, Z. Deng, J. Tian and T. Liu, *Eur. J. Med. Chem.*, 2017, **127**, 900–908.

10 L. Y. Ma, L. P. Pang, B. Wang, M. Zhang, B. Hu, D. Q. Xue, K. P. Shao, B. L. Zhang, Y. Liu, E. Zhang and H. M. Liu, *Eur. J. Med. Chem.*, 2014, **86**, 368–380.
11 H. N. Li, H. Wang, Z. P. Wang, H. N. Yan, M. Zhang, Y. Liu and M. S. Cheng, *Bioorg. Med. Chem.*, 2018, **26**, 4025–4033.
12 L. Zhao, L. Mao, G. Hong, X. Yang and T. Liu, *Bioorg. Med. Chem. Lett.*, 2015, **25**, 2540–2544.
13 S. Narsimha, K. N. Satheesh, S. B. Kumara, R. M. Vasudeva, H. S. K. Althaf and R. M. Srinivasa, *Bioorg. Med. Chem. Lett.*, 2016, **26**, 1639–1644.
14 P. V. Chavan, U. V. Desai, P. P. Wadgaonkar, S. R. Tapase, K. M. A. Choudhari and D. Sarkar, *Bioorg. Chem.*, 2019, **85**, 475–486.
15 R. Al-Salahi, M. Marzouk, A. Gamal Eldeen, A. Alanazi, M. Al-Omar and M. Fouda, *J. Pure Appl. Microbiol.*, 2013, **7**, 189–198.
16 R. Al-Salahi, A. E. Elsayed, R. E. M. Wadaan, E. Ezzeldin and M. Marzouk, *Lat. Am. J. Pharm.*, 2016, **35**, 58–65.
17 R. Al-Salahi, A. E. Elsayed, R. E. M. Wadaan, E. Ezzeldin and M. Marzouk, *Lat. Am. J. Pharm.*, 2016, **35**, 66–73.
18 R. Al-Salahi, M. Marzouk, A. Ashour and I. Alswiadan, *Asian J. Chem.*, 2014, **26**, 2173–2176.
19 R. Al-Salahi, R. Ahmad, E. Anouar, N. N. I. Iwana, M. Marzouk and H. A. Abuelizz, *Future Med. Chem.*, 2018, **10**, 1889–1905.
20 H. Abuelizz, R. Al-Salahi, J. Al-Asri, J. Mortier, M. Marzouk, E. Ezzeldin, A. A. Ali, M. G. Khalil, G. Wolber, H. A. Ghabbour, A. A. Almehizia and G. A. Abdel Jaleel, *Chem. Cent. J.*, 2017, **11**, 103.
21 R. Al-Salahi, K. E. Tahir, N. Lolak, M. Hamidaddin, I. Alswaidan and M. Marzouk, *Chem. Cent. J.*, 2014, **8**, 3.
22 R. Al-Salahi, I. Alswaidan, M. Al-Omar and M. Marzouk, *Life Sci. J.*, 2013, **10**, 2018–2028.
23 R. Al-Salahi and D. Geffken, *Synth. Commun.*, 2011, **41**, 3512–3523.
24 R. Al-Salahi and D. Geffken, *Molecules*, 2010, **15**, 7016–7034.
25 A. S. Hassan, M. F. Mady, H. M. Awad and T. S. Hafez, *Chin. Chem. Lett.*, 2017, **28**, 388–393.
26 A. N. Emam, S. A. Loutfy, A. A. Mostafa, H. M. Awad and M. B. Mohamed, *RSC Adv.*, 2017, **7**, 23502–23514.
27 E. M. Flefel, W. A. El-Sayed, A. M. Mohamed, W. I. El-Sofany and H. M. Awad, *Molecules*, 2017, **22**(170), 1–13.
28 R. Gerl and D. L. Vaux, *Carcinogenesis*, 2005, **2**, 263–270.
29 M. Khan, A. Maryam, J. I. Qazi and T. Ma, *Int. J. Biol. Sci.*, 2015, **16**, 1100–1112.

